Virgo and the gravitational interferometry

Maddalena Mantovani[1,*] for the Virgo Collaboration

[1]European Gravitational Observatory (EGO), I-56021 Cascina, Pisa, Italy

Abstract. The Advanced Virgo detector is a long scale enhanced Michelson interferometer placed in Italy, close to Pisa, with the aim of detecting gravitational waves from astronomical sources. The Advanced Virgo interferometer has detected, together with the LIGO interferometers located in USA [1], an impressive collection of gravitational waves emissions in the last observation runs O2 and O3. During the last observation run (O3), which lasted about one year of data taking from April 2019 to March 2020, were detected about 80 events. When the run ended, the detector has been upgraded toward the Advanced Virgo + configuration, in order to enhance its sensitivity, which it is currently in the commissioning phase. After an introduction on gravitational wave detection, the paper will focus on giving an overview of the evolution of the Virgo antenna in the past decades.

1 Introduction and gravitational wave detection principle

The gravitational waves (GWs) have been predicted in 1916 by Albert Einstein [2] as quadrupole emissions creating ripples in the space-time due to extremely violent astrophysics events (e.g. supernova explosions, collisions of neutron stars and black holes, etc...). Due to the weak interaction between the gravitational waves and the matter, their direct detection occurred only one century after the prediction.
The technological advancements allowed the LIGO-Virgo collaboration to detect the GW emission from two coalescing black holes on the 14^{th} of September 2015 (GW150914) [3].
As it has been mentioned before, the GW modifies the space-time metric in a quadrupole way, which means that modifies the distance measured between free-falling masses in a differential way for orthogonal directions. For this reason the most promising detection principle results to be the use of a Michelson interferometer, detecting the GW passage as a deviation from the interference condition [4]. The change of differential length due to a GW signal of strain amplitude h measured by a Michelson interferometer having orthogonal arms with length L is equal to::

$$\Delta L = \frac{hL}{2} \tag{1}$$

In order to have an idea of the order of magnitude of the observable displacement, it can be considered that for an arm length of 1 km the GW having a strain amplitude of 10^{-22} the generated displacement is very small of the order of $\Delta L = 10^{-19}$ m.
For this reason the optical configuration of the GW detector is much more complex than a simple Michelson interferometer.

*e-mail: μ maddalena.mantovani@ego-gw.it

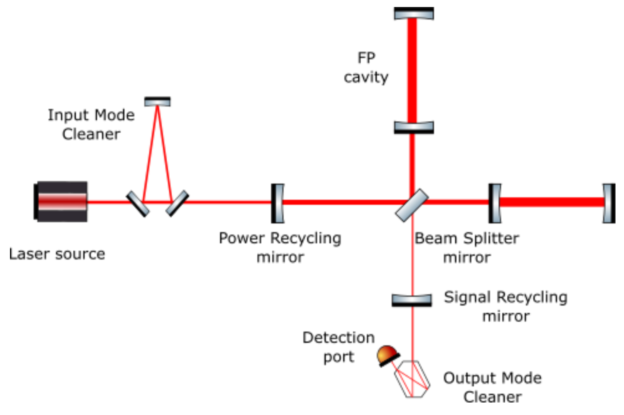

Figure 1. Schematic drawing of the Virgo detector in which the main optical components are shown as: the Fabry-Perot cavities (FP cavities), 3km long orthogonal arms, the Power Recycling mirror (PR), the Signal recycling mirror (SR), the Beam Splitter mirror (BS) which splits the incoming beam generated by the laser source in the two cavities and defines the interference condition at the detection port. Moreover two additional cavities are implemented to clean and stabilize the input and output beam, the Input Mode Cleaner (IMC) and the Output Mode Cleaner (OMC) respectively.

Additional cavities are added to enhance the detector response to GW signals, as shown in Figure 1:

- the Fabry-Perot cavities in the long arms. The addition of a high reflecting mirror in the long arm allows to have the laser beam to bounce between the two mirrors increasing the laser power stored in the cavity, to reduce the Shot-Noise limit of the sensitivity, and to increase the optical path length of the arm.
- the Power Recycling mirror (PR). The addition of the PR between the laser and the interferometer increases the recycled light to improve the Shot-Noise limit.
- the Signal Recycling mirror (SR). The SR mirror is placed between the Beam-Splitter mirror (BS) and the detection port to recycle the GW signal enhancing the detector response.

The addition of all these optical resonators allowed to improve the detector sensitivity up to the first detection of GW emission in 2015, but on the other hand the increase of complexity of the detector has strongly increased the difficulties in its commissioning. The main reason is that the detector provides the best sensitivity only if all the optical cavities are actively controlled to maintain precise resonant conditions [1][5][6].
Moreover, the sensitivity of the detector is not limited only by the Quantum-Noise (Radiation pressure and Shot Noises), but also other fundamental noises contribute to the sensitivity, such as the thermal noise [2] and the seismic noise. The technological enhancements pushed these limits towards unprecedented levels.

2 The Virgo detector and its evolution

The Virgo experiment has been started in 1997 thanks to a French-Italian collaboration [7]. The Virgo collaboration has grown in time, being currently a collaboration formed by 800

[1] In order to have an idea of the accuracy requirements of the control on the position of the main optical component it can be said that the differential displacement of the two long arms has to be lower than 10^{-16} m.

[2] The thermal noise is due to the thermal excitation of the mechanical modes of the test masses and the suspensions, resulting in a spurious signal at the detection port

	Virgo	Advanced Virgo	Advanced Virgo+
Input power [W]	17	25	33
FP *Finesse*	50	450	450
Arm cavity geometry	Plano-Concave	quasi-confocal	quasi-confocal
Power Recycling gain	50	38	38
Signal Recycling			✓
Fused silica fibers	for VSR3	✓	✓
Scientific joint runs	VSR1, VSR2, VSR3	O2, O3	spring 2023
Maximum BNS range [Mpc]	17	60	
GW detection		✓	

Table 1. Summary table to show the main parameters of the Virgo detectors.

members, 534 authors, 136 institutions from 15 countries. The installation and commissioning of the Virgo detector was completed in June 2006 [8], the main optical parameters are listed in the first column of Table 1 1 [3]. For the first time three scientific runs had been carried out in coincidence with the LIGO detectors, namely VSR1, from March to October 2007, and VSR2, from July to December 2009 and the last VSR3, from June to October 2011. The major change between the VSR2 configuration and the VSR3 is the modification of the bottom part of the payload by substituting the steel wires hanging the test masses with fused silica fibers, in order to kill the suspension thermal noise.
The mean BNS range [4] achieved by the Virgo detector in the VSR3 run was about 17 Mpc. Unfortunately the sensitivity reached in the VSR* runs was not enough to allow a GW detection.
After the end of the VSR3 observing run, the detector has been upgraded toward the Advanced Virgo experiment [11]. The long arm cavity geometry has been strongly changed, from plano-concave to quasi-confocal configuration, to reduce the test mass thermal noise. Moreover to improve the Shot-noise and to increase the optical path length the arm finesse has been strongly increased of a factor 9 respect to the Virgo configuration, see second column of Table.
The strong increase of the power stored in the arm cavities, and the marginality of the recycling cavity stability, has lead to strong effort in developing and implementing a Thermal Compensation system (TCS) to cope with thermal transients and defects [12]. The Advanced Virgo experiment allowed to detect on the 14^{th} August 2017 the first triple coincidence LIGO/Virgo, BH-BH merging GW170814. Only few days later, on the 17^{th} of August, the first detection of binary neutron star system occurred. The detection has lead to an intense observing campaign in the electromagnetic follow-up [13]. The O2 and O3 runs contributed to detect more than 80 GW events.
The O3 observing run was concluded in March 2020, at the beginning of the pandemic emergency, the scientific data taking period was stopped to start the installation of the Advanced Virgo+ experiment.
The main differences between the Advanced Virgo+ and the Advanced Virgo detector [14] are (see third column of Table 1):

- addition of the Signal recycling mirror, see Figure 1, to improve the detector response

[3] The *Finesse* of an Fabry-Perot cavity is a parameter which defines how narrow the resonance is, and it is proportional to the cavity gain which is the ratio between the stored power and the input power [10].

[4] The BNS range is defined as the distance at which a bynary system of two neutrons stars (having 1.4 solar masses each) could be detected with a signal to noise ratio of 8.

- increase of the input power, to reduce the quantum noise at high frequency (shot-noise)
- addition of frequency dependent squeezing [15], to improve the broadband quantum noise

The installation of the Advanced Virgo+ has been concluded in December 2020, after that the detector entered in the commissioning phase to put in operation the aforementioned upgrades. The interferometer has been commissioned for almost two years, reaching a stable operability of the detector. Now it is currently in the phase of optimization and noise hunting to achieve the design sensitivity to start the O4 joint run, in the spring of 2023.
The main detector parameters for the three Virgo configurations are summarized in Table 1.

3 Conclusions

The Virgo detector, together with the LIGO ones, has evolved in time reaching unprecedented sensitivities allowed to open a new window on the universe by detecting a impressive large amount of GW emissions.
The detector is currently in the Advanced Virgo+ configuration which is meant to start the scientific data taking, in a joint run, in the next spring.

References

[1] Aasi J et al. (LIGO Scientific Collaboration) 2015 Class. Quant. Grav. 32 074001
[2] Einstein, A.; Die Grundlage der allgemeinen Relativitatstheorie, Ann. Phys. 49, 769-822, 1916.
[3] Abbott, R. et al. (LIGO Scientific Collaboration and Virgo Collaboration); Observation of Gravitational Waves from a Binary Black Hole Merger. Phys. Rev. Lett.,116, 061102, 2016.
[4] Nardecchia, I. Detecting Gravitational Waves with Advanced Virgo. Galaxies 2022, 10, 28. https://doi.org/10.3390/galaxies10010028
[5] Acernese, F.; et al. The Advanced Virgo longitudinal control system for the O2 observing run. Astropart. Phys. 2020, 116, 102386.
[6] Allocca, A., et al. "Interferometer Sensing and Control for the Advanced Virgo Experiment in the O3 Scientific Run". Galaxies 2020, 8, 85. https://doi.org/10.3390/galaxies8040085
[7] "VIRGO - Final Design Report" - https://dcc.ligo.org/T970234/public
[8] T. Accadia, et al. "Status of the Virgo project" Class. Quantum Grav. 28 (2011) 114002
[9] J. Abadie *et al.* VIRGO and LIGO Scientific collaboration, "Sensitivity Achieved by the LIGO and Virgo Gravitational Wave Detectors during LIGO's Sixth and Virgo's Second and Third Science Runs," [arXiv:1203.2674 [gr-qc]].
[10] A.E. Siegman, ", University Science Books, Mill Valley, 1986
[11] The Virgo collaboration, "Advanced Virgo Technical Design Report" https://tds.virgo-gw.eu/ql/?c=18777
[12] L Aiello et al 2019 J. Phys.: Conf. Ser. 1226 012019
[13] Abbott, B. P.; et al. (LIGO, Virgo and other collaborations) (October 2017). The Astrophysical Journal. 848 (2): L12. arXiv:1710.05833
[14] The Virgo Collaboration, 'Advanced Virgo Plus Phase I Design Report', Virgo-Technical Documentation System, Report No. VIR-0596A-19 (2019) https://tds.virgo-gw.eu/ql/?c=14430
[15] Jean-Pierre Zendri, et al. 'Advanced Virgo Squeezer Technical Design Report' LVK internal note, https://tds.virgo-gw.eu/ql/?c=11140, VIR-0411C-15